Desalination and Water Treatment
www.deswater.com

37(2012)277–287
January

1944-3994/1944-3986 © 2012 Desalination Publications. All rights reserved
doi: 10/5004/dwt.2012.2745

Taylor & Francis
Taylor & Francis Group

Modelling the transient behaviour of a fixed bed considering both intra and inter-pellet diffusion for adsorption of parachloro-meta-xylenol (PCMX)

Sudeshna Saha[a], Ujjaini Sarkar[b,*], Sourav Mondal[a]

[a]*Department of Applied Sciences, University of Quebec at Chicoutimi, 555 boul. de l'Université, Chicoutimi, QC, Canada G7H 2B1*
[b]*Department of Chemical Engineering, Jadavpur, Jadavpur University, Jadavpur, Kolkata-700032, West Bengal, India*
Tel./Fax: +91-33-24146378; email: abhi_nandan47@rediffmail.com

Received 22 February 2011; Accepted 21 July 2011

ABSTRACT

Phenols and Phenolics are considered to be potentially hazardous water pollutants. Parachloro-metaxylenol (PCMX) is the major component of several disinfectants, produced commercially by well-known pharmaceutical companies. Adsorption of PCMX in various combinations of adsorbents, both natural and artificial, has been studied. Specially, water hyacinth (Eichhornia crassipes [Mart] Solms-Laubach) stems were used as adsorbent in combination with powdered activated carbon (PAC) and granular activated carbon (GAC). Five equilibrium isotherm models, namely, Tempkin Isotherm, Freundlich Isotherm, Langmuir Isotherm, Redlich-Peterson Isotherm and Toth Isotherm were studied and parameterized. The dynamics of fixed-bed adsorption columns for modeling is a demanding task due to the strong nonlinearities in the equilibrium isotherms, interference effects of the competition of solutes for adsorbent sites, mass transfer resistances between fluid phase and solid phase and fluid-dynamic dispersion phenomena. A mathematical model has been studied for a fixed bed isothermal adsorption column with porous adsorbent. Simulations were carried out to understand the specific influence of inter-pellet diffusion and external film resistance. The effect of flow rate, bed length and initial concentration of adsorbate were studied. Rapid occurrence of breakthrough time was observed for higher flow rates of effluent, lower bed height and high initial concentration of effluent.

Keywords: Pharmaceutical waste water; Water hyacinth; Parachloro-metaxylenal; Dynamic simulation; Intra pellet diffusion; Breakthrough

1. Introduction

Phenol and its corresponding substituted compounds are important environmental pollutants because of their toxic effects towards life in the aquatic environment even when present in small concentrations as demonstrated by Mbui et al. and I. Polaert [1,2].

Phenol and its vapors are corrosive to the eyes, the skin, and the respiratory tract [3]. Repeated or prolonged skin contact with phenol may cause dermatitis, or even second and third-degree burns due to phenol's caustic and defatting properties [4]. Inhalation of phenol vapor may cause lung edema, affects the central nervous system and heart, resulting in dysrhythmia, seizures, and coma [3,5]. Repeated exposure of phenol may have harmful effects on the liver and kidneys [6]. The major mechanism for the toxicity of phenol, other than its hydrophobic character, may be the formation of phenoxyl radicals [7].

Several potential sources of phenolic compounds have been widely used in industry and agriculture and this has led to the classification of phenol itself and ten other substituted phenols by the United States

*Corresponding author.

Environmental Protection Agency (USEPA) as priority pollutants. Phenol is classified as a 'Class B' poison by the interstate commission, reported by Mbui et al. [1]. Phenolics are key components of the effluents from coke production, coal gasification, pharmaceuticals, pesticides, fertilizers, dye manufacturing, synthetic chemicals, pulp and paper industries. According to the US EPA maximum concentration level of total phenolic compounds in the treated industrial effluent and water supplies should be less than 1 μg/ml [8]. The permissible limit of phenol and phenolics for the treated industrial effluents is 1 mg/l as mentioned by Central Pollution Control Board (CPCB), India [9]. Therefore it seems to be extremely important to remove the PCMX from water and wastewater before its transport and cycling into the natural environment. This in turn poses real challenges for the developing countries to evolve efficient techniques for their removal.

Water Hyacinth is a perennial aquatic herb (Eichhornia crassipes) which belongs to the family Pontedericeae, closely related to the Liliaceae (lily family). The mature plant consists of long, pendant roots, rhizomes, stolons, leaves, inflorescences and fruit clusters. The plants are up to 1 m high although 40 cm is the more usual height. The inflorescence bears 6–10 lily-like flowers, each 4–7 cm in diameter. The stems and leaves contain air-filled tissue which give the plant its considerable buoyancy and also make the stems suitable for physical adsorption of some water borne toxic materials. Wolverton and McKown report that the water hyacinth (Eichhornia crassipes [Mart] Solms-Laubach) is a large, free-floating, tropical aquatic plant [10]. Water hyacinths grow most rapidly in water temperatures ranging from 28°C to 30°C and at a pH in the range of 4.0 to 8.0. They cease to grow when water temperature is above 40° or below 10°C, and the pH range for growth is below 4.0. On many occasions it has been demonstrated that this weed is excellent for the removal of pollutants for domestic waste water. Abdel-Halim et al. reports that the percent removal of lead was 100% by bone powder, 90% by active carbon, 80% by plant powder from water hyacinth and 50% by commercial carbon [11]. A study by Kruatrachue et al. demonstrates the phytoremediation potential of water hyacinth (*Eichhornia crassipes)*, for the removal of cadmium (Cd) and zinc (Zn) [12]. Removal of Chlorophenols from waste water by bio-film and biofilm components has been reported in many literatures [13,14].

The dynamics of fixed-bed adsorption columns for modeling is a demanding task due to the strong nonlinearities in the equilibrium isotherms, interference effects of the competition of solutes for adsorbent sites, mass transfer resistances between fluid phase and solid phase, and fluid-dynamic dispersion phenomena. The interaction of these effects produces steep concentration fronts, which move along the column during the adsorption process. This has to be accounted for while modeling the system. Most of the reported studies on adsorptive separation have been related to the equilibrium and kinetic studies and their adsorption behaviours as a single component as well as multi-component systems [15–24]. Adsorbents used were activated carbon, molecular sieves and sometimes specially developed adsorbents. These studies discussed the mass transfer mechanism, adsorptive capacities of the adsorbents, suitability of the type of isotherm to represent the equilibrium and effects of parameters controlling the dynamics of the system. Bed performances with respect to geometry, physical and operating parameters need to be attempted, including the mechanism of the process and concentration histories. Pore and solid diffusion models for fixed bed adsorbers were developed by Weber and Chakravorti [25]. Kucukosmanoglu et al. have studied the adsorption behaviors of Methylene Blue and Methyl Orange on a diaminoethane sporopollenin (DAE-S) solid phase [26]. Such investigations were performed in a column arrangement, and breakthrough profiles were used in evaluations and quantifications. Removal of PCMX by dried and dead water hyacinth stems has been attempted for the first time in a packed bed column (operated continuously) in this research work. Batch equilibrium analysis by Sadhukhan et al. is appealing and forms the basis for the design of the packed column [27]. Here, the adsorption behaviors were evaluated using some standard adsorption isotherm models. A number of well known isotherm models (e.g., Tempkin Isotherm, Freundlich Isotherm, Langmuir Isotherm, Redlich-Peterson Isotherm and Toth Isotherm) have been discussed and the parameters of five different adsorption isotherms were estimated using a robust non-linear least square scheme, based on chi-squared minimization, established by Levenberg and Marquardt. The uncertainties on the estimated parameters were computed, along with the range of confidence limits. Later, these models were ranked according to their performance, based on minimum χ^2.

Simulations were carried out to understand the influence of axial dispersion, radial diffusion, interpellet diffusion and external film resistance on adsorption using the above model. The partial differential equations were solved simultaneously using the *pdepe* function of MATLAB 7.0, based on various finite difference schemes. The effect of flow rate, bed height and initial concentration of adsorbate was studied. Rapid occurrence of breakthrough time was observed for higher flow rates of effluent, lower bed height and high initial concentration of effluent.

2. Experimental methods

These were thoroughly washed to remove mud and any other dirt particles. These were then dried under the sunlight for 3–4 d. These were cut into small cylindrical pieces and thus became ready to be used for the experiment with no specified size. All the reagents used were of analytical grade and their solutions were made up in ultra pure water (HPLC Grade Water, filtered through 0.2 micron filters, maximum absorbance 0.204 at 210 nm, Make: Ranchem, India). Specifically the PCMX standards were made from pharmaceutical grade PCMX of Reckitt and Benckiser (India) Ltd. A 330–900 nm wavelength spectrophotometer (Make: PERKIN ELMER, Model: PRECISELY LAMDA 25 UV/Visible) equipped with a standard 10 nm path length sample cell was used for absorption measurement of PCMX. An accumet silver–silver combination pH electrode (Model 15, Fischer Scientific, and USA) was used for pH measurements.

The apparatus for dynamic study comprised of a storage tank, a pumping arrangement, a distribution system and a packed-bed adsorption column (see Fig. 1). The inlet of the adsorption column was equipped with a distribution system in order to get uniform flow across the cross section of the adsorption column and also to minimize the effect of channeling. The distributor had 0.5 mm diameter pores throughout the cross section. The distribution system comprised of a rotating head arrangement in order to measure the flow rate and also to load and unload the packing material in the adsorption column. The column was packed with aquatic macrophytes (water hyacinth stems), activated charcoal and sand usually in the ratio of 2:1:1.5. However we used three different compositions of the bed (A, B and C), and these were chosen after several batch experiments.

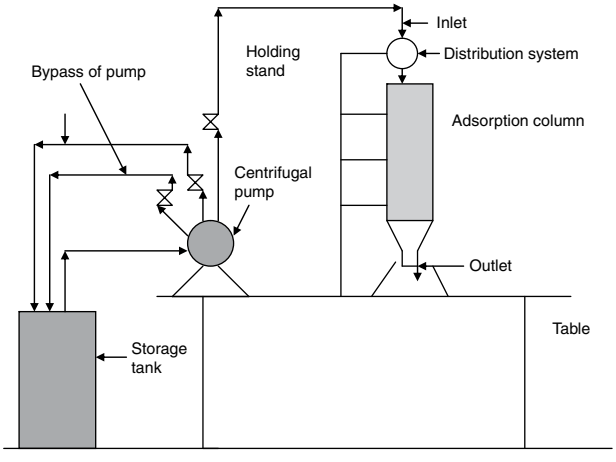

Fig. 1. Experimental setup for the dynamic study.

The column was loosely packed as the dried aquatic macrophytes were swollen with the absorption of water and thus the void fraction of the column decreased with time. The effluent coming out from the column was collected at regular intervals and analyzed for the concentrations of the PCMX in the spectrophotometer using standard analytical protocol. The experiments were carried out at different flow rates, feed concentrations and bed heights without changing the ratio of the adsorbents. Only in certain experiments, necessary for the validation of the mathematical model, different compositions of the bed were used. The inside diameter of the fixed bed column is 8 cm. The bed heights were varied from 8.5 cm to 18 cm.

3. Modeling

Fig. 2 and Fig. 3 represent the front view and top view of the two dimensional differential control volume of the composite fixed bed respectively.

The one-dimensional solute transport model in the fixed bed (which describes the adsorption dynamics) is described by the convection-diffusion model.

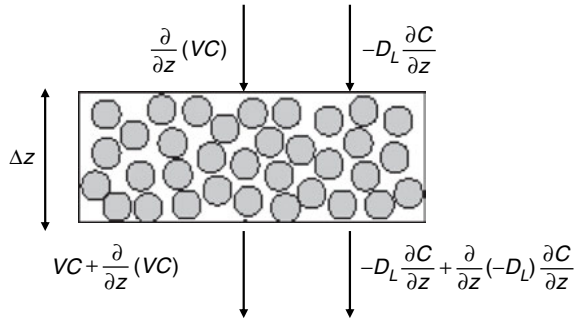

Fig. 2. 2-D Representation of the differential control volume of the composite fixed bed (Front View).

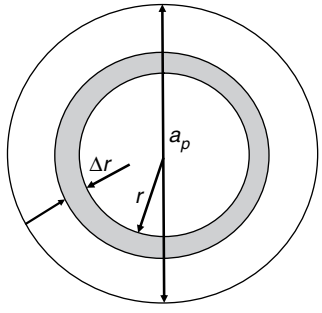

Fig.3. 2-D Representation of the differential control volume of the composite fixed bed (Top View).

The overall mass balance gives:

Accumulation = Output – Input + Generation due to mass transfer

Generation term: $\rho_s \frac{(1-\varepsilon)}{\varepsilon}\frac{\partial q}{\partial t}$, where $\frac{\partial q}{\partial t}$ is the fluid-solid mass transfer rate. The mass transfer is based on the linear difference in the concentration gradient $\frac{\partial q}{\partial t} = \frac{3k_f}{a_p}(C - C_e)$

Accumulation term: $\frac{\partial C}{\partial t}$

Now making a mass balance in the differential section Δz, and on rearranging, we get:

$$\frac{\partial C}{\partial t} = D_L \frac{\partial^2 C}{\partial z^2} - V\frac{\partial C}{\partial z} - \left(\frac{3k_f}{a_p}\right)\frac{(1-\varepsilon)}{\varepsilon}\rho_s (C - C_e) \quad (1)$$

Eq. (1) represents the variation of solute concentration in the adsorber bed, with respect to space and time.

The above equation is based on the following assumptions:

1. Flow is one-dimensional in the vertical direction and uniform across the cross-sectional area.
2. The bed is fully saturated, (i.e., all interparticle voids are filled with liquid).
3. There is negligible mass transfer resistance on the liquid side.
4. The velocity of the liquid phase is constant along the column.
5. The adsorbent particles are spherical and homogenous in size and density.
6. The void fraction of the column decreased with time.

The initial conditions considered are given by:

$$C = C_0, \; z = 0 \quad (2)$$

$$C = 0, \; 0 < z < L \quad (3)$$

The boundary conditions at both ends of the column are:

$$D_L \frac{\partial C}{\partial z} = -V(C_0 - C) \text{ at } z = 0, \; t > 0 \quad (4)$$

$$\frac{\partial C}{\partial z} = 0 \text{ at } z = L, t \geq 0 \quad (5)$$

3.1. Intra-Pellet adsorption

The intra-pellet adsorption is governed by the pore diffusion transport model. Intra–particle mass transport is due to Fickian diffusion, and is characterized by the pore diffusion coefficient D_p. The mass balance equation for the liquid phase (pore) in a spherical particle can be written as:

$$\varepsilon_p \frac{\partial C_p}{\partial t} + (1-\varepsilon_p)\rho_s \frac{\partial q}{\partial t} = D_p\left(\frac{\partial^2 C_p}{\partial r^2} + \frac{2}{r}\frac{\partial C_p}{\partial r}\right) \quad (6)$$

Here ε_p is the particle porosity; C_p is solute concentration inside the particle.

Assuming instantaneous equilibrium is given by

$$\frac{\partial q}{\partial t} = \frac{\partial C_p}{\partial t}\frac{\partial q}{\partial C_p} \quad (7)$$

Modifying the Eq. (6) using the above equation, we obtain the following equation.

$$\frac{\partial C_p}{\partial t} = \frac{1}{\left[1 + \rho_s\left(\frac{1-\varepsilon_p}{\varepsilon_p}\right)\frac{\partial q}{\partial t}\right]}\left(\frac{D_p}{\varepsilon_p}\right)\left(\frac{\partial^2 C_p}{\partial r^2} + \frac{2}{r}\frac{\partial C_p}{\partial r}\right) \quad (8)$$

The initial condition considered is given by

$$C_p = 0, \quad 0 < r < a_p, \quad t = 0 \quad (9)$$

The symmetry condition at the centre of the particles and the condition of continuity on the external surface of the adsorbent bed are expressed simultaneously by:

$$\frac{\partial C_p}{\partial r} = 0, \quad r = 0, \quad t > 0 \quad (10)$$

$$k_f(C_p - C_e) = D_p\varepsilon_p \frac{\partial C_p}{\partial r}, \quad r = a_p, \quad t > 0 \quad (11)$$

3.2. Adsorption isotherms

Table 1 demonstrates various adsorption isotherms along with the parameterized ecoefficients.

The solution algorithm was done with the help of MATLAB 7.0 using the *pdepe* function. The *pdepe* function is useful in solving such initial value boundary partial differential equation in one dimensional space–time system.

pdepe solves PDEs of the form:

$$c\left(x, t, u, \frac{\partial u}{\partial x}\right)\frac{\partial u}{\partial t} = x^{-m}\frac{\partial}{\partial x}\left(x^m f\left(x, t, u, \frac{\partial u}{\partial x}\right)\right) + s\left(x, t, u, \frac{\partial u}{\partial x}\right) \quad (12)$$

Table 1
Parameter estimation and uncertainty analysis

Sample	Model	k_1	k_2	d.f.	χ^2	$\rho(\chi^2)$	Uncertainties on		RANK	95% Confidence limits (k_1)		95% Confidence limit (k_2)	
							k_1	k_2		Lower	Upper	Lower	Upper
ADRB1	1	1.4412	0.3460	8	6.3635	0.3934	0.0037	0.0014	1	1.4296	1.4528	0.3414	0.3506
	2	1.6300	1.0442	8	217.8541	1.000	0.0399	0.0274	4	1.5056	1.7543	0.9587	1.1297
	3	1.6769	0.1851	8	7.0906	0.4731	0.0248	0.0065	3	1.5995	1.7543	0.1647	0.2055
	4	0.3629	0.2007	8	690.5615	1.000	219.9534	654.3190	5	−684.6781	685.4038	−2037.6644	2038.0657
	5	1.7838	0.2129	8	6.7481	0.4359	0.0324	0.0083	2	1.6827	1.8849	0.1869	0.2389
ADRB2	1	1.6531	0.3941	6	11.5901	0.9282	0.0178	0.0077	1	1.5976	1.7087	0.3699	0.4182
	2	1.7294	0.8670	6	199.9912	1.000	0.0779	0.0305	2	1.4865	1.9723	0.7719	0.9621
	3	0.3629	0.2007	6	388.8946	1.000	0.0856	0.0892	4	0.0961	0.6296	−0.0771	0.4785
	4	0.3629	0.2007	6	489.3833	1.000	540.6232	2118.0153	5	−1683.3985	1684.1242	−6596.3203	6596.7216
	5	0.3629	0.2007	6	385.7939	1.000	0.0892	0.0883	3	0.0849	0.6408	−0.0743	0.4757
ADRB3	1	0.3629	0.2006	8	1.1468	0.0028	0.0031	0.0037	1	0.3531	0.3726	0.1889	0.2123
	2	0.3850	0.9240	8	1.4034	0.0058	0.0121	0.0981	3	0.3472	0.4228	0.6183	1.2297
	3	2.3721	5.2417	8	1.3384	0.0049	126.0131	318.9120	2	−390.0936	394.8380	−988.0041	998.4876
	4	0.4104	−0.1281	8	4.0930	0.1513	71.8360	267.3928	5	−223.3217	224.1425	−832.9183	832.6620
	5	1.2026	1.9784	8	1.5882	0.0088	5.9189	12.0456	4	−17.2318	19.6372	−35.5374	39.4943

The PDEs hold for $t_0 \le t \le t_f$ and $a \le x \le b$. The interval $[a, b]$ must be finite. m can be 0, 1, or 2, corresponding to slab, cylindrical, or spherical symmetry, respectively.

In the above equation, $f(x, t, u, \partial u/\partial x)$ is a flux term and $s(x, t, u, \partial u/\partial x)$ is a source term. The coupling of the partial derivative with respect to time is restricted to multiplication by a diagonal matrix $c(x, t, u, \partial u/\partial x)$.

For $t = t_0$ and all x, the solution components satisfy initial conditions of the form

$$u(x, t_0) = u_0(x) \tag{13}$$

For all t and either $x = a$ or $x = b$, the solution components satisfy a boundary condition of the form

$$p(x, t, u) + q(x, t) f\left(x, t, u, \frac{\partial u}{\partial x}\right) = 0 \tag{14}$$

The command line statement *sol=pdepe(m,@pdefun, @icfun,@bcfun,xmesh,tspan)* solves initial-boundary value problems for systems of parabolic and elliptic PDEs in the one space variable and time. The ordinary differential equations (ODEs) resulting from discretization in space were integrated to obtain approximate solutions at times specified in *tspan*. The pdepe function returned values of the solution on a mesh provided in *xmesh. @pdefun, @icfun* and *@bcfun* are function handles to the *pdepe*, the initial condition and the boundary condition respectively.

In the solution of the above PDE [Eq. (1)],

$$m = 0; \tag{15}$$

$$c = 1; \tag{16}$$

$$f = D_L \frac{\partial C}{\partial z} \tag{17}$$

$$s = -\left[V \frac{\partial C}{\partial z} + \left(\frac{3k_f}{a_p} \right) \frac{(1 - \varepsilon)}{\varepsilon} \rho_s \left(C - C_e \right) \right] \tag{18}$$

$$C(0, 0) = C_0 \text{ and } C(L,0) = 0 \tag{19}$$

$$\text{At } z = 0,\ p = V(C_0 - C) \text{ and } q = 1 \tag{20}$$

$$\text{At } z = L,\ p = 0 \text{ and } q = \frac{1}{D_L} \tag{21}$$

Similarly for the solution of the Eq. (8) the set of the variable declaration was done and hence the equations were simultaneously solved to produce the required output within the boundaries of the experiment. The arrays of *zmesh* and *tspan* were appropriately defined to generate the profile of solute concentration distribution in the adsorber bed. The values of other parameters have been experimentally determined and are henceforth used in the simulation of the model.

4. Results and discussion

PCMX is the major component of the very popular antiseptic DETTOL. We expect the untreated effluent of

the DETTOL Plant to contain very high levels of PCMX (in the range of 100 ppm to 400 ppm depending on the rate of production). We attempted to remove this PCMX by physical adsorption using various combinations of natural adsorbents. Experiments were carried out to obtain the adsorption equilibrium data to parameterize five popular isotherms [27]. Later a fixed bed adsorption system was designed to treat the plant effluent continuously. Following composition profiles were maintained.

Composition A: Water hyacinth 62 g, charcoal 31 gm, sand 46.5 gm.

Composition B: Water hyacinth 42 g, charcoal 21 gm, sand 31.5 gm.

A pore diffusion model was developed including intra-pellet adsorption. Various scenarios were simulated dynamically. These included variations in flow rate, bed height and initial feed concentration.

4.1. Results of the batch equilibrium study

Morphology of Water Hyacinth stems was done using Scanning Electron Microscope (Make: JEOL; Model: JSM 5800) at three different resolutions (Refer Fig. 4a and Fig. 4b). Surface area of the water hyacinth stems has been measured by BET method (Make: Quantachrome; Model: NOVA 40003). BET surface area of the sample has been found to be 19.54 m^2/g with Nitrogen as the adsorbate, as compared to that of tea factory waste being 0.30 m^2/g, xanthated chitosan being 0.49 m^2/g and that of lead monoxide powder being 0.25 m^2/g [28–30]. Fig. 4a and Fig. 4b clearly reveal the surface texture, flocs, and different levels of porosity in the water hyacinth stems under study. Parameter estimation results are given in Table 1 where the uncertainties and confidence intervals of each parameter are presented for each of the models for various samples.

The Tempkin isotherm yields the best fit for all the samples, having performed better than Freundlich Isotherm. Model 1(based on Tempkin Isotherm) was ranked 1 in case of all the 3 samples.

4.2. Effect of changing flow rate

The results for different feed flow rates are plotted for an average bed height of 19.5 cm and an inlet adsorbate concentration of 137.79 mg/l and 178.82 mg/l respectively in Fig. 5 and Fig. 6. It shows that as the flow rate increases from 1.23 to 2.7 ml/sec, the breakthrough curve becomes steeper. The experimental break point time decreases from 85 (Fig. 5) to 50 min (Fig. 6). Corresponding breakpoints are observed at 80 and 45 min respectively with the modeled data. This is quite expected if we take into account the relatively higher time needed to reach adsorption equilibrium with material of the composite fixed bed. Indeed, the higher the flow rate, the lower is the contact time between the solute and the substrate. So at high flow rate the adsorbate solution leaves the column before achieving equilibrium. Furthermore, a fixed saturation capacity of the bed, based on the same driving force, gives rise to a shorter time for saturation at higher flow rate. The variation of flow rate leads to variations in turbulence inside the bed interstices affecting the mass transfer rate. It is also observed from the figures that with decrease in flow-rate, the breakthrough occurs late and there is almost a proportionate increase in breakthrough time with the decrease in flow-rate.

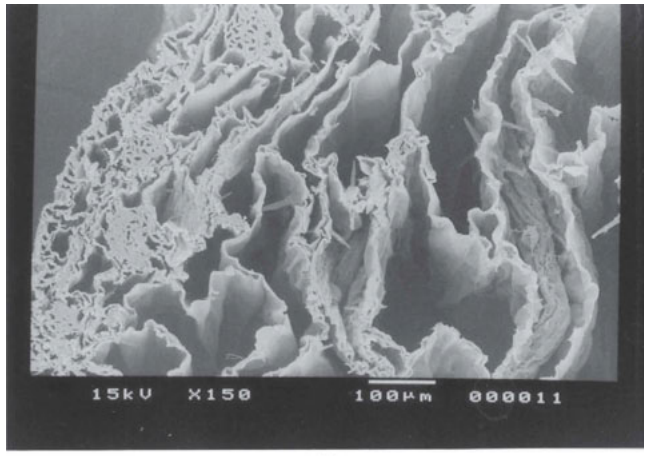

(a)

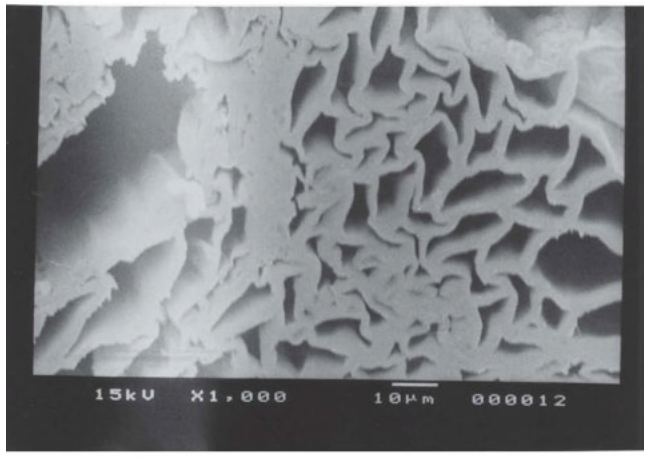

(b)

Fig. 4. Scanning electron micrograph of Water Hyacinth (*E. crassipes)* Stem.

4.3. Effect of changing bed height

The effect of bed height on the effluent adsorbate concentration is presented in Fig. 7 for a bed height of

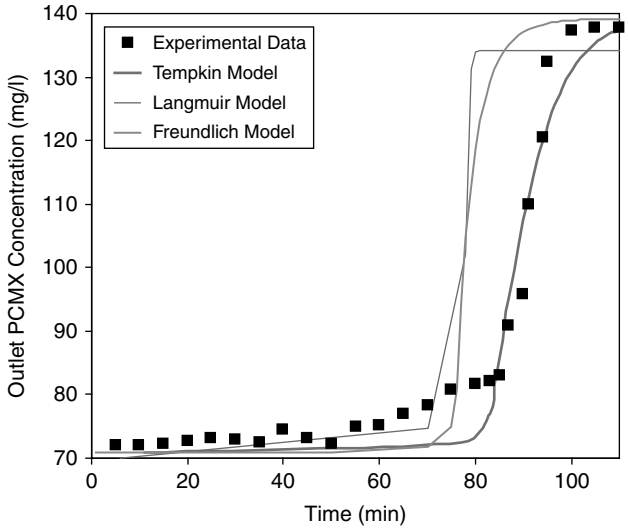

Fig. 5. Temporal variation of PCMX Concentration at the bed outlet (mg/l) with Initial Feed Concentration = 137.79 mg/l; Average Bed Height = 19.5 cm; Flow rate V_0=1.23 ml/s; Bed Composition: *A*.

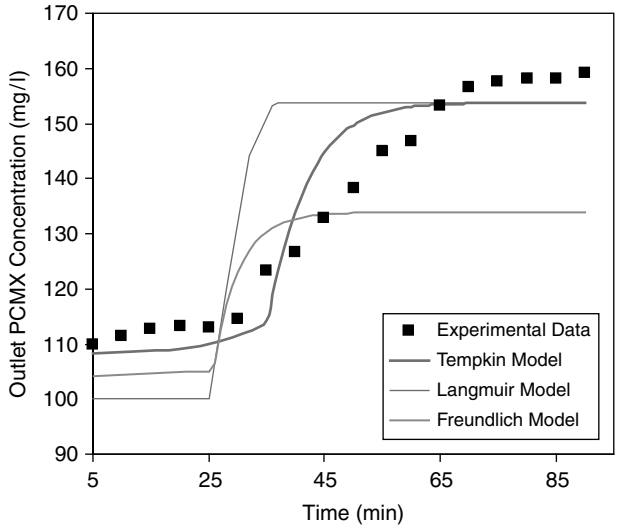

Fig. 7. Temporal variation of PCMX Concentration at the bed outlet (mg/l) with Initial Feed Concentration = 160.0 mg/l; Average Bed Height = 10.5 cm; Flow rate V_0=1.23 ml/s; Bed Composition: *A*.

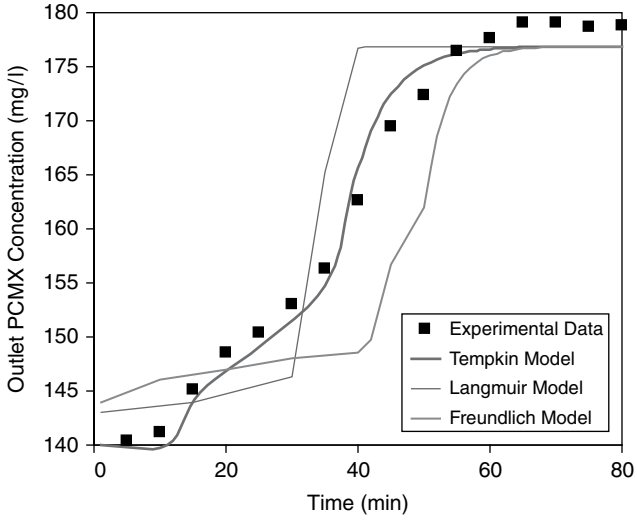

Fig. 6. Temporal variation of PCMX Concentration at the bed outlet (mg/l) with Initial Feed Concentration = 178.82 mg/l; Average Bed Height = 19.5 cm; Flow rate V_0=2.7 ml/s; Bed Composition: *A*.

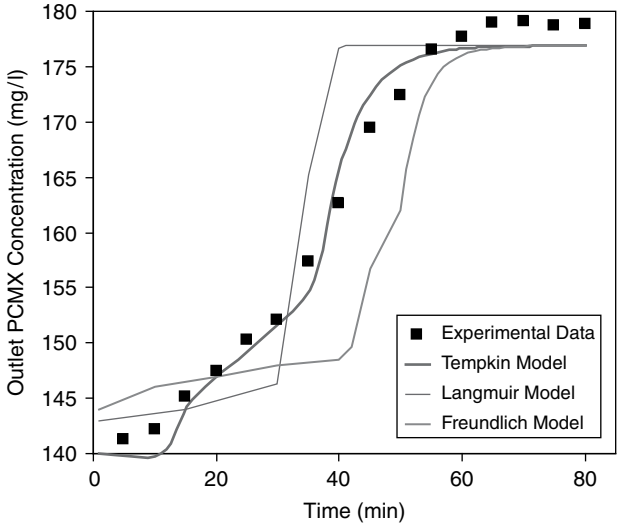

Fig. 8. Temporal variation of PCMX Concentration at the bed outlet (mg/l) with Initial Feed Concentration = 178.82 mg/l; Average Bed Height = 19.5 cm; Flow rate V_0=1.23 ml/s; Bed Composition: *A*.

10.5 cm, flow rate of 1.23 ml/s and inlet adsorbate concentration of 160.0 mg/l and in Fig. 8 for a bed height of 19.5 cm, a flow rate of 1.23 ml/s and inlet adsorbate concentration of 178.82 mg/l. It is observed that with the increase in bed height from 10.5 cm to 19.5 cm, the experimental break point time increases from 28 to 35 min. Corresponding breakpoints are observed at 35 and 37 min respectively with the modeled data. This shows that the bed is saturated in less time for smaller bed heights. A shorter bed length implies a smaller capacity of the bed to adsorb the adsorbate from solution and hence a faster increase in the rate of adsorption. For a longer bed the mass transfer zone would be contained within the bed. In such cases the concentration breakthrough curves would remain unchanged with change in the bed length. The effect of bed length would be prominent for shorter bed lengths due to the axial dispersion within the beds. The inflow rate would affect these scenarios immensely.

4.4. Effect of changing initial concentrations

The effect of inlet adsorbate concentration on effluent concentration is shown in Fig. 9 and Fig. 10. Other parameters such as bed height and flow rate were kept constant. It was observed that as the inlet adsorbate concentration decreased from 178.82 to 174.10 mg/l, the experimental break point time increased from 25 to 40 min.

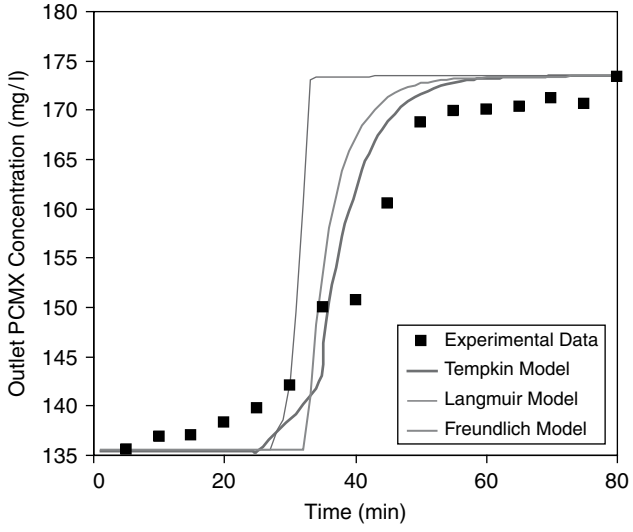

Fig. 9. Temporal variation of PCMX Concentration at the bed outlet (mg/l) with Initial Feed Concentration = 174.10 mg/l; Average Bed Height = 19.5 cm; Flow rate V_0= 2.7 ml/s; Bed Composition: A.

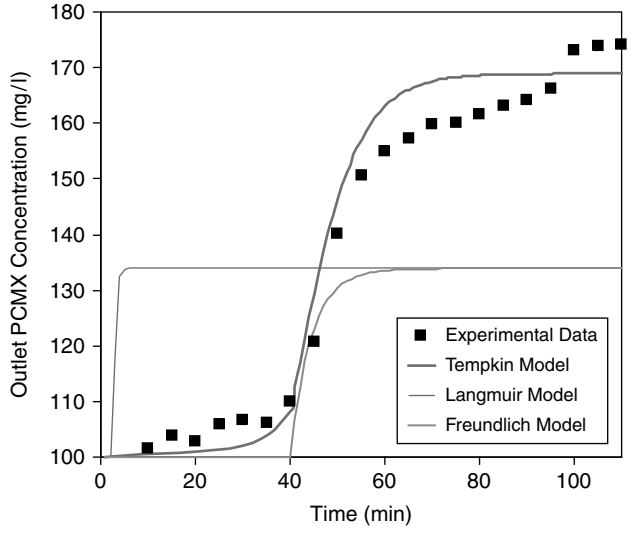

Fig. 10. Temporal variation of PCMX Concentration at the bed outlet (mg/l) with Initial Feed Concentration = 174.10 mg/l; Average Bed Height = 19.5 cm; Flow rate V_0 = 1.23 ml/s; Bed Composition: A.

Corresponding breakpoints are observed at 35 and 25 min respectively with the modeled data. For larger feed concentration, steeper breakthrough curves are found, because of the lower mass-transfer flux from the bulk solution to the particle surface due to the weaker driving force. In addition, at high concentration, the isotherm gradient is smaller, yielding a higher driving force along the pores. Thus the equilibrium was attained faster for higher adsorbate concentration. Early concentration breakthroughs, with higher inlet concentration may be attributed to the fact that higher liquid phase PCMX concentration increases the mass transfer rate at the early stage of adsorption and is expected to get early and steep breakthrough.

In the simulation program we have assumed that the entire length is used up for adsorption from the beginning. However, it did not happen in practice. One part of the bed length remained unused at the beginning, while rapid adsorption took place when the entire bed came in contact with the solution. Overall mass transfer coefficient, k is defined here as the surface area per unit volume of water hyacinth. It is indicative of strong or poor adsorptivity of adsorbent. It may be improved either by making bigger pore sizes, facilitating mechanism of transport or by improving the adsorbate-adsorbent affinity through surface modification.

5. Conclusions

A dynamic adsorption study was carried out on the removal of PCMX from wastewater using a composite adsorbent bed containing both natural and artificial adsorbents. Water-hyacinth appeared to be very effective in removing the PCMX from the effluent. Equilibrium results were modeled and evaluated using five different isotherms and the well known Levenburg-Marquardt parameter estimation method, based on the χ^2minimization. Tempkin isotherm gave the best fit. As flow rate increased, the breakthrough curves became steeper. The experimental break point time matched very well with the modeled ones. It was also observed from the figures that decrease in flow-rate caused late breakthrough and there was almost a proportionate increase in breakthrough time with the decrease in flow-rate. For larger feed concentrations, steeper breakthrough curves were obtained due to lower mass-transfer flux from the bulk solution to the particle the driving force being weaker. Early concentration breakthroughs, with higher inlet concentration, might be attributed to the higher mass transfer rate due to higher liquid phase PCMX concentration at the early stage of adsorption resulting in steep breakthrough.

Though the model simulation results were successfully validated with the experimental data, more experiments should be carried out. This would require measurements accounting the extreme variations in flow rate, bed heights, bed composition and initial concentration. It would also be essential to determine unacceptable end effects in the column that account for such variability in order to have a firm basis for developing guidelines for operating such columns under specific bounds.

Appendix I

I.1. Models for adsorption isotherms

I.1.1. The tempkin isotherm (Model 1)

Tempkin considered the effects of some indirect adsorbate/adsorbate interactions on adsorption isotherms suggested that the heat of adsorption of all the molecules in the layer would decrease linearly with coverage due to these interactions [31]. The Tempkin isotherm has been used in the following form:

$$q = k_2 \log C + k_1 \quad \textbf{(I.1)}$$

Here q is the equilibrium solid phase concentration in mg per 100 ml per gm of adsorbent C is the equilibrium liquid phase concentration in mg per 100 ml. The constant k_1 is related to the heat of adsorption.

I.1.2. The freundlich isotherm (Model 2)

The Freundlich expression assumes that the adsorbate concentration increases along with the concentration of adsorbate on the adsorbent surface:

$$q = k_1 (C)^{k_2} \quad \text{(I.2)}$$

In this equation k_1, k_2 are the Freundlich constants. This expression is characterized by the heterogeneity factor, k_2 so this isotherm may be used to describe various heterogeneous systems [32,33]. The Freundlich equation agrees well with the Langmuir equation over moderate concentration ranges but, unlike the Langmuir expression, it does not reduce to the linear isotherm (Henry's law) at low surface coverage. Both these theories suffer from the disadvantage that equilibrium data over a wide concentration range cannot be fitted with a single set of constant.

I.1.3. The langmuir isotherm (Model 3)

The theory for Langmuir isotherms assumes a monolayer coverage of adsorbate over a homogenous adsorbent surface. Therefore, at equilibrium, a saturation point is reached where no further adsorption can occur adsorption takes place at specific homogeneous sites within the adsorbent. In the following equation, k_1, k_2 are the Langmuir constants:

$$q = \frac{k_1 C}{k_2 + C} \quad \text{(I.3)}$$

I.2. Parameter estimation (Cabrera and Grau, 2006)

The nonlinear Levenburg-Marquardt parameter estimation method, as described in the function LMF of MATLAB Version 7.0 was used to obtain the parameters in each of the three models described in equations 1 till 3. In this method, we usually define a merit function, SSQ (Sum of the SQuares of the deviations) and determine the best-fit parameters by its minimization. Given a set of empirical data pairs of independent and dependent variables, (x_i, y_i), we optimize the parameters β of the model curve $f(x, \beta)$ so that the sum of the squares of the deviations become minimal.

$$S(\beta) = \sum_{i=1}^{m} \left[y_i - f(x_i, \beta) \right]^2 \quad \text{(I.4)}$$

The parameters are iteratively adjusted, due to nonlinear dependences, to minimize the SSQ in order to achieve a global minimum. We start with a set of trial values for the parameters to be estimated, which are gradually improved. The procedure is then repeated until the SSQ effectively stops decreasing. A sensitivity matrix was derived for the three models for the adsorption function (amount adsorbed/unit amount of adsorbent used versus equilibrium Cr (VI) concentration) with respect to the parameters k_1 and k_2.

The gradient matrix can be written as:

For Model 1:

$$\frac{\partial q}{\partial k_1} = 1.0 \quad \text{(I.1a)}$$

$$\frac{\partial q}{\partial k_2} = \log C \quad \text{(I.1b)}$$

For Model 2:

$$\frac{\partial q}{\partial k_1} = C^{k_2} \quad \text{(I.2a)}$$

$$\frac{\partial q}{\partial k_2} = k_1 C^{k_2} \log C \quad \text{(I.2b)}$$

For Model 3:

$$\frac{\partial q}{\partial k_1} = \frac{C}{(k_2 + C)} \quad \text{(I.3a)}$$

$$\frac{\partial q}{\partial k_2} = -\frac{k_1 C}{(k_2 + C)^2} \quad \text{(I.3b)}$$

I.3. Evaluation of the three models

Evaluation of the following statistical parameters is necessary if we need to infer on the estimated parameters:

1. The minimized SSQ function, $S(\beta)$ as given in Eq. (1), which is the least-squares measure of the fit (the smallest SSQ gives the best model).
2. The uncertainties associated with the estimate of each parameter, formally termed as the standard error σ. These are the square-root of the error term covariance matrix C_{ij} of the fit. The closer this value is to zero, the better the fit.
3. The correlation coefficient (r^2). The higher the %, better is the fit.

Symbols

a_p	—	equivalent particle diameter of the adsorbent particle (m)
C	—	effective solute concentration (mg/l)
C_p	—	Solute concentration inside the pore (mg/l)
C_e	—	equilibrium solute concentration (mg/l)
D_L	_	effective dispersion coefficient (m^2/s)
D_p	—	effective pore diffusivity (m^2/s)
k_1	—	Constant of the equilibrium isotherm models
k_2	_	Constant of the equilibrium isotherm models
k_f	—	external mass transfer co – efficient (m/s)
Q	—	weight of the solute adsorbed per unit weight of adsorbent (mg/g)
r	—	local variable radius of the particle (m)
T	—	time (min)
V	—	superficial velocity of the solution through the bed (m/s)
ε	—	bed porosity
ε_p	—	particle porosity
ρ_s	—	particle density (kg/m^3)

References

[1] D.N. Mbui, P.M. Shiundu, R.M. Ndonye and G.N. Kamau, Adsorption and detection of some phenolic compounds by rice husk ash of Kenyan origin, J. Environ. Monit., 4 (2002) 978–984.

[2] I. Polaert, A.M. Wilhelm and H. Delmas, Phenol wastewater treatment by a two-step adsorption–oxidation process on activated carbon, Chem. Eng. Sci., 57 (2002) 1585–1590.

[3] S. Budavari, ed. (1996), The Merck Index: An Encyclopedia of Chemical, Drugs, and Biologicals. Whitehouse Station, NJ: Merck.

[4] T.M. Lin, S.S. Lee, C.S. Lai and S.D. Lin (June 2006). "Phenol burn", Burns: Journal of the International Society for Burn Injuries, 32(4) 517–521521. doi:10.1016/j.burns.2005.12.016. PMI D 16621299.

[5] M.A. Warner and J.V. Harper, "Cardiac dysrhythmias associated with chemical peeling with phenol". *Anesthesiology* 62(3) (1985) 366–7. doi:10.1097/00000542–198503000–00030. PMID 2579602.

[6] World Health Organization/International Labour Organization: International Chemical Safety Cards, http://www.ilo.org/public/english/protection/safeworkkcis/products/icsc/dtasht/icsc00/icsc0070.htm.

[7] Hanscha, Corwin; McKarnsb, Susan C; Smith, Carr J; Doolittle, David J (June 15, 2000), "Comparative QSAR evidence for a free-radical mechanism of phenol-induced toxicity". Chemico-Biological Interactions, 127(1) 61–72. doi:10.1016/S0009–2797(00)00171-X. PMID 10903419.

[8] http://www.epa.gov/waterscience/standards/rules/ntr.html#sectionG3.

[9] CPCB, 1995.General guidelines for discharge of effluents. (Inland surfacewater).

[10] B.C. Wolverton and M.M. McKown, Water Hyacinths for removal of Phenols from polluted waters, Aquatic Botany, 2 (1976) 191–201.

[11] S.H. Abdel-Halim, A.M.A. Shehata and M.F. El-Shahat, Removal of lead ions from industrial waste water by different types of natural materials, Water Res., 37 (2003) 1678–1683.

[12] X. Lu, M. Kruatrachue, P. Poketchitiyook and K. Homyok, Removal of Cadmium and Zinc by water hyacinth, Eichhornia Crassipes, Science Asia, 30 (2004) 93–103.

[13] W. Wang, X. Zhang and D. Wang, Adsorption of p-chlorophenol by biofilm components, Water Res., 36 (2002) 551–560.

[14] P.M. Armenante, L.S. Colella, D. Kafkewitz and M.J. Larkin, Effect of a biofilm on the adsorption of 4-chlorophenol on activated carbon, Appl. Microbiol. Biotechnol., 46 (1996) 667–672.

[15] S.D. Manjare and A.K Ghoshal, Studies on Dynamic adsorption behavior of Ethyl Acetate from air on 5A & 13X molecular sieves, Can. J. Chem. Eng., 83(2) (2005) 232–241.

[16] S.D. Manjare and A.K. Ghoshal, Adsorption equilibrium studies for ethyl acetate vapor and E-Merck 13X molecular sieve system, Sep. Purif. Technol., 51 (2006) 118–125.

[17] E.C. Moretti, Reduce VOC and HAP emissions, Chem. Eng. Prog., 98 (2002) 30–40.

[18] A. Adak and A. Pal, Removal of phenol from aquatic environment by SDS-modified alumina: Batch and fixed bed studies, Sep. Purif. Technol., 50 (2006) 256–262.

[19] C.A. Grande, C. Gigola and A.E. Rodrigues, Adsorption of Propane and Propylene in pellets and crystals of 5A zeolite, Ind. Eng. Chem. Res., 41 (2002) 85–92.

[20] M.C. Huang, C.H. Chou and H. Teng, Pore size effects on activated carbon capacities for volatile organic carbon adsorption, AIChE J., 48 (2002) 1804–1809.

[21] A. Chong Lua and Q. Jia, Adsorption of phenol by oil–palm-shell activated carbons in a fixed bed, Chem. Eng. J., 150 (2009) 455–461.

[22] Y.A. Alhamed, Adsorption kinetics and performance of packed bed adsorber for phenol removal using activated carbon from dates' stones, J. Hazard. Mater.,170 (2009) 763–770.

[23] Y. Suyadal, M. Erol and H. Oguz, Deactivation model for adsorption of TCE vapor on an activated carbon bed, Ind. Eng. Chem. Res., 39 (2000) 724–730.

[24] V.K. Gupta and N. Verma, Removal of volatile organic compounds by cryogenic condensation followed by adsorption, Chem. Eng. Sci., 57(14) (2002) 2679–2696.

[25] T.W. Weber and R.K. Chakravorti, Pore and Solid Diffusion Models for fixed bed adsorbers, AIChE J., 20 (1974) 228–238.

[26] M. Küçükosmanoğlu, Gezici and A. Ayar, The adsorption behaviors of Methylene Blue and Methyl Orange in a diaminoethane sporopollenin-mediated column system, Sep. Purif. Technol., 52 (2006) 280–287.
[27] S. Sadhukhan, S. Singha and U. Sarkar, Adsorption of para chloro meta xylenol (PCMX) in composite adsorbent beds: Parameter estimation using nonlinear least square technique, Chem. Eng. J., 152 (2009) 361–366.
[28] E. Malkoc and Y. Nuhoglu, "Fixed bed studies for the sorption of chromium(VI) onto tea factory waste", Chem. Eng. Sci., 61 (2006) 4363–4372.
[29] N. Sankararamakrishnan, P. Kumar and V. Singh Chauhan, "Modeling fixed bed column for cadmium removal from electroplating wastewater", Sep. Purif. Technol., 63 (2008) 213–219.
[30] A. Jena and K. Gupta, "A novel technique for surface area and particle size determination of component of fuel cell & batteries", Porous Materials, Inc. Cornell Business & Technology Park, 83 Brown Road, Ithaca, NY 14850.
[31] M.J. Tempkin and V. Pyzhev, Acta. Physiochim. URSS, 12 (1940) 217.
[32] H. Moon and W.K. Lee, Intraparticle Diffusion in liquid phase adsorption of phenols with activated carbon in finite batch adsorber, J. Colloid Interface Sci., 96 (1983) 162–170.
[33] B. Al-Duri and G. McKay, Basic Dye Adsorption on Carbon Using a Solid-Phase Diffusion Model, Chem. Eng. J., 38 (1988) 23–31.